Chemistry–A European Journal
Research Article
doi.org/10.1002/chem.202200034
Chemistry Europe
European Chemical Societies Publishing
www.chemeurj.org

Metal-Organic Frameworks as Unique Platforms to Gain Insight of σ-Hole Interactions for the Removal of Organic Dyes from Aquatic Ecosystems

Cristina Negro[+],[a] Paula Escamilla[+],[a] Rosaria Bruno,[b] Jesus Ferrando-Soria,*[a] Donatella Armentano,*[b] and Emilio Pardo*[a]

Abstract: The combination of high crystallinity and rich host-guest chemistry in metal-organic frameworks (MOFs), have situated them in an advantageous position, with respect to traditional porous materials, to gain insight on specific weak noncovalent supramolecular interactions. In particular, sulfur σ-hole interactions are known to play a key role in the biological activity of living beings as well as on relevant molecular recognitions processes. However, so far, they have been barely explored. Here, we describe both how the combination of the intrinsic features of MOFs, especially the possibility of using single-crystal X-ray crystallography (SCXRD), can be an extremely valuable tool to gain insight on sulfur σ-hole interactions, and how their rational exploitation can be enormously useful in the efficient removal of harmful organic molecules from aquatic ecosystems. Thus, we have used a MOF, prepared from the amino acid *L*-methionine and possessing channels decorated with $-CH_2CH_2SCH_3$ thioalkyl chains, to remove a family of organic dyes at very low concentrations (10 ppm) from water. This MOF is able to efficiently capture the four dyes in a very fast manner, reaching within five minutes nearly the maximum removal. Remarkably, the crystal structure of the different organic dyes within MOFs channels could be determined by SCXRD. This has enabled us to directly visualize the important role sulfur σ-hole interactions play on the removal of organic dyes from aqueous solutions, representing one of the first studies on the rational exploitation of σ-hole interactions for water remediation.

Introduction

Weak noncovalent interactions are ubiquitous in many relevant processes occurring in livings beings, and represent one of the most important tools in Supramolecular Chemistry to mimic/emulate such processes.[1–4] Among them, σ-hole interactions are of particular interest. A σ-hole is the region of electron deficiency that appears in the outer lobe of an orbital, when an atom from the group V–VII -with half-filled *p* orbitals-, participate in a covalent bond.[5–7] This σ-hole can create a region of positive electrostatic potential -if the rest of the molecule presents a relatively sufficient electron-withdrawing nature with respect to the group V–VII atom, and this one is sufficiently polarizable- able to interact with electron donors, such as nitrogen and oxygen, and even, π-systems. Despite this interaction is present in key supramolecular recognitions processes and is very relevant in biological activity, it has been somehow underestimated in comparison to hydrogen-bonds, with the exception of halogen ones.[7] For example, this is the case of sulfur σ-hole interaction, which it has been mainly described in post-analysis of close contacts in protein data bank or as stabilizing agent of desired conformations of drugs to interact with receptors.[8–12] Indeed, the rational use of such interaction for specific applications has been barely explored.[13–20]

Metal-organic frameworks (MOFs)[21–28] are a class of crystalline porous inorganic-organic materials, whose rich host-guest chemistry[29–35] and high crystallinity,[36–38] together with the possibility to have -to a certain extent- a control of their dimensionality, topology and functionality by chemical design,[39–45] have situate them in an advantageous position with respect to other porous materials. This has been clearly exemplified by the continuous growth of novel aesthetically pleasant crystal structures,[46–49] as well as by the wide range of applications where they have shown successful, for example gas storage and separation, catalysis, drug delivery, conductivity, molecular recognition of small molecules, encapsulation of functional moieties, magnetism, chemical nanoreactors and water remediation.[50–62] Indeed, relevant advances performed in

[a] C. Negro,[+] P. Escamilla,[+] Dr. J. Ferrando-Soria, Dr. E. Pardo
Instituto de Ciencia Molecular (ICMOL), Universitat de València
Paterna 46980, València (Spain)
E-mail: jesus.ferrando@uv.es
emilio.pardo@uv.es

[b] R. Bruno, Dr. D. Armentano
Dipartimento di Chimica e Tecnologie Chimiche
Università della Calabria
87030, Rende, Cosenza (Italy)
E-mail: donatella.armentano@unical.it

[+] These authors contributed equally to this work.

Supporting information for this article is available on the WWW under https://doi.org/10.1002/chem.202200034

MOFs' chemistry have been, mainly, consequence of the combined possibility to tailor the functionalities decorating MOFs channels by chemical design and the application of single-crystal X-ray diffraction (SCXRD) as basic characterization tool.[63–68] This has demonstrated as a powerful approach to understand/rationalize host-guest interactions and, eventually, to find, structure-properties relationships that have enabled positive feedback of knowledge to develop more performant MOFs.[69] Thus, MOFs are, *a priori*, excellent playgrounds to gain insight on specific molecular recognitions interactions, such as sulfur σ-hole, with the intention to exploit them towards a targeted application.

Contamination of aquatic ecosystems with organic dyes represents a severe environmental problem, having a negative impact on the quality of aquatic ecosystems -i.e. inhibiting plants and algae photoactivity and representing a health threat for fish, as a consequence of their teratogenic, mutagenic and carcinogenic character- and consequently on human life.[70] Different technologies have been studied for the removal of organic dyes from wastewater streams.[71–73] Among them, the use of water-resistant highly stable MOFs[74,75] for their capture and/or photodegradation has revealed as a very promising approach.[71,76–79] This is mainly due to the intrinsic characteristic properties of MOFs highlighted above. However, despite the great structural, compositional and functional diversity of MOFs, their potential has been poorly explored and somehow underdeveloped in this field. Thus, more research efforts are needed to fully unleash them.

One of our research lines is focused on exploiting the differentiating features of MOFs toward catalytic and water remediation applications.[52,71] Along the development of our investigations, we have found that sulfur σ-hole interactions[13-20] may have a more prominent role in the capture process than previously thought. In this context, we aim to expand our knowledge on these interactions through the rational application of suitable MOFs for the removal of organic dyes from aquatic ecosystems. To this end, we have prepared a neutral 3D MOF, with formula $\{Sr^{II}Cu_6^{II}[(S,S)\text{-methox}]_3(OH)_2(H_2O)\}\cdot 16H_2O$ (**1**; methox = bis[(*S*)-methionine]oxalyl diamide), constructed with oxamato ligands derived from the natural amino acid *L*-methionine (see Experimental Section, Supporting Information).[13,14,18,19] The selection of **1** was not accidental. This was based on our previous work with an isoreticular MOF to **1** -with calcium instead of strontium.[13,14] This MOF exhibited functional channels decorated with flexible $-CH_2CH_2SCH_3$ thioalkyl chains with outstanding molecular recognition properties -for a variety of heavy metals and organic contaminants like neonicotinoid insecticides- and high crystallinity -which have enabled to unveil the crystal structure of diverse and unique host-guest assemblies.[15,18] In this work, we have observed that **1** is capable to remove, efficiently, four organic dyes -that are commonly used as antiseptics in hospitals or in textile industries- (Auramine O (AO), Brilliant Green (BG), Methylene Blue (MB) and Pyronin Y (PY)) at very low concentrations (10 ppm) from water (Scheme S1). Indeed, this process takes place with a very fast kinetics, improving, notably, the performance of a related reported MOF with serine hydroxyl-residues functionalizing the pores,[80] which, *a priori*, would be expected to interact more efficiently with organic molecules through hydrogen-bonds. Thanks to the high degree of crystallinity of **1**, and the application of cutting-edge single-crystal X-ray crystallography techniques, we have been able to get unique snapshots of the assembled host–guest systems, which have allowed to rationalize the nice removal efficiency of **1**, and more importantly, improve our knowledge on sulfur σ-hole interaction.

Results and Discussion

Removal Experiments of Organic Dyes

In order to evaluate the removal efficiency of **1** toward the four selected organic dyes -Auramine O (AO), Brilliant Green (BG), Methylene Blue (MB) and Pyronin Y (PY)- we processed **1** in the form of extruded pellets, by mixing polycrystalline powders of **1** with commercial Matrimid in 80:20 ratios (Experimental Section, Supporting Information). The structuration of MOFs is a very interesting and necessary topic of research, which allows to prepare materials with improved applicability as a direct consequence of their better handling and longer lifetime.[81] However, in some cases, it is difficult to retain the chemical/physical properties of the selected MOF. To rule out this, we have performed PXRD of **1** structured as pellets, which evidence that is isostructural to polycrystalline powders of **1** (Figure S1a,b).

Then, using **1** as pellets (50 mg), we have studied the removal efficiency of **1** for four organic dyes using individual spiked solutions of each of them (10 mL, 10 ppm) in real water samples from Turia river (Valencia, Spain). These processes were followed with UV-vis spectroscopy (Figures 1 and 2), measuring the decrease in the intensity of the respective characteristic/principal absorption band in the visible region at different times (1, 5, 30, 60, 360 and 720 min). The obtained kinetic profile (Figure 2 and Table S2) evidenced the efficient and fast adsorption of all four tested dyes, reaching nearly 90% of removal after only 5 min. This contrast with the serine-based MOF, which need nearly 24 h to reach the same capture efficiency.[80] This removal efficiency and kinetics of adsorption was even maintained when using a multi-dye mixture solution, 10 ppm of each of all four dyes (Figure S2, Table S3 and Experimental Section, Supporting Information). Here, it is noteworthy to remark the relevance of the observed results by **1**, which not only is capable to capture these organic contaminants at very low concentration -similar to the ones found in industrial wastewaters- in a very efficient and fast manner, but also in samples where the presence of other ions could interfere the adsorption process.

The pH-dependence of the capture properties of **1** has been also evaluated. Thus, the same capture experiments above described were repeated, but adjusting the pH at 5 and 11, with HCl and NaOH, respectively (Figures S3–S6). Overall, the capture efficiency in both acid and basic media are almost

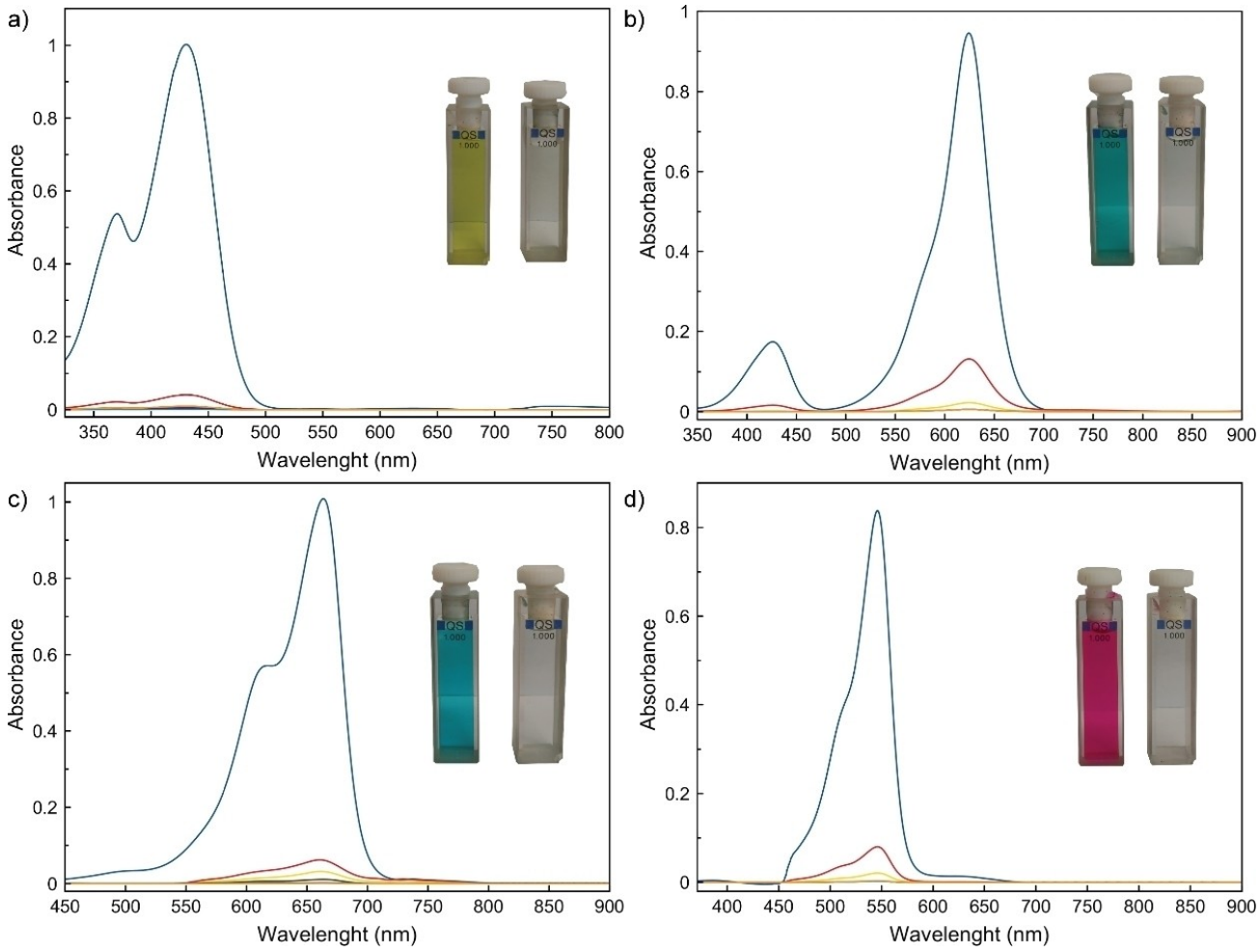

Figure 1. Evolution with time of the UV-Vis absorption spectra of 10 ppm solutions of AO (a), BG (b), MB (c) and PY (d) in real water samples from Turia river when using 50 mg of pellets of **1** as adsorbent. Colors code: Blue: $t=0$; Red: $t=1$ min.; Yellow: $t=5$ min.; Orange $t=30$ min.; Light blue $t=360$ min.; Green: $t=720$ minutes. The inset shows the photographs of the solutions at $t=0$ (left) and after only five minutes of the dye removal experiments (right).

identical to that observed with real water samples, suggesting that **1** is equally effective under moderate changes in pH.

Recyclability, maximum uptake and scale-up

In order to fully characterize a material, and think toward real-world applications, the reusability and structural and physical integrity are parameters of main relevance. We observed **1** could be easily regenerated, by immersing the extruded pellets in a methanol solution for 15 min, while retaining the crystallinity -as PXRD in Figure S1c evidenced- and maintaining the removal efficiency in the next capture experiment (Table S4). The crystallinity was also retained for **1** after capture experiments at pH = 5 and 11 and the same regeneration treatment, as PXRD shows (Figure S1d,e). Further evidence of the robustness of the extruded pellets of **1** was assessed by scanning electron microscopy (SEM). Figure S7 shows the final appearance of pellets of **1** before and after the capture-regeneration process.

Aiming to evaluate the maximum loading capacity of **1** for each organic dye, we immersed **1** for two weeks in aqueous saturated solutions of each dye, while replacing the saturated solution every 12 h. Maximum uptakes of 598.9, 786.8, 554.0 and 542.6 mg g^{-1} were obtained for AO, BG, MB and PY, respectively (see Experimental Section for characterization details). These values were obtained from the CHSN analyses gathered in Table S5. Overall, these features, together with the easiness to produce **1** at multigram-scale (see Experimental Section, Supporting Information) and environmentally benign nature of its components, makes **1** an attracting candidate to be tested in pilot plants or structured in mixed-matrix membranes.

X-ray Crystal Structure

In order to elucidate the host–guest interactions established between **1** (structure shown in Figure 3) and the captured organic dyes -playing special attention to sulfur σ-hole ones-,

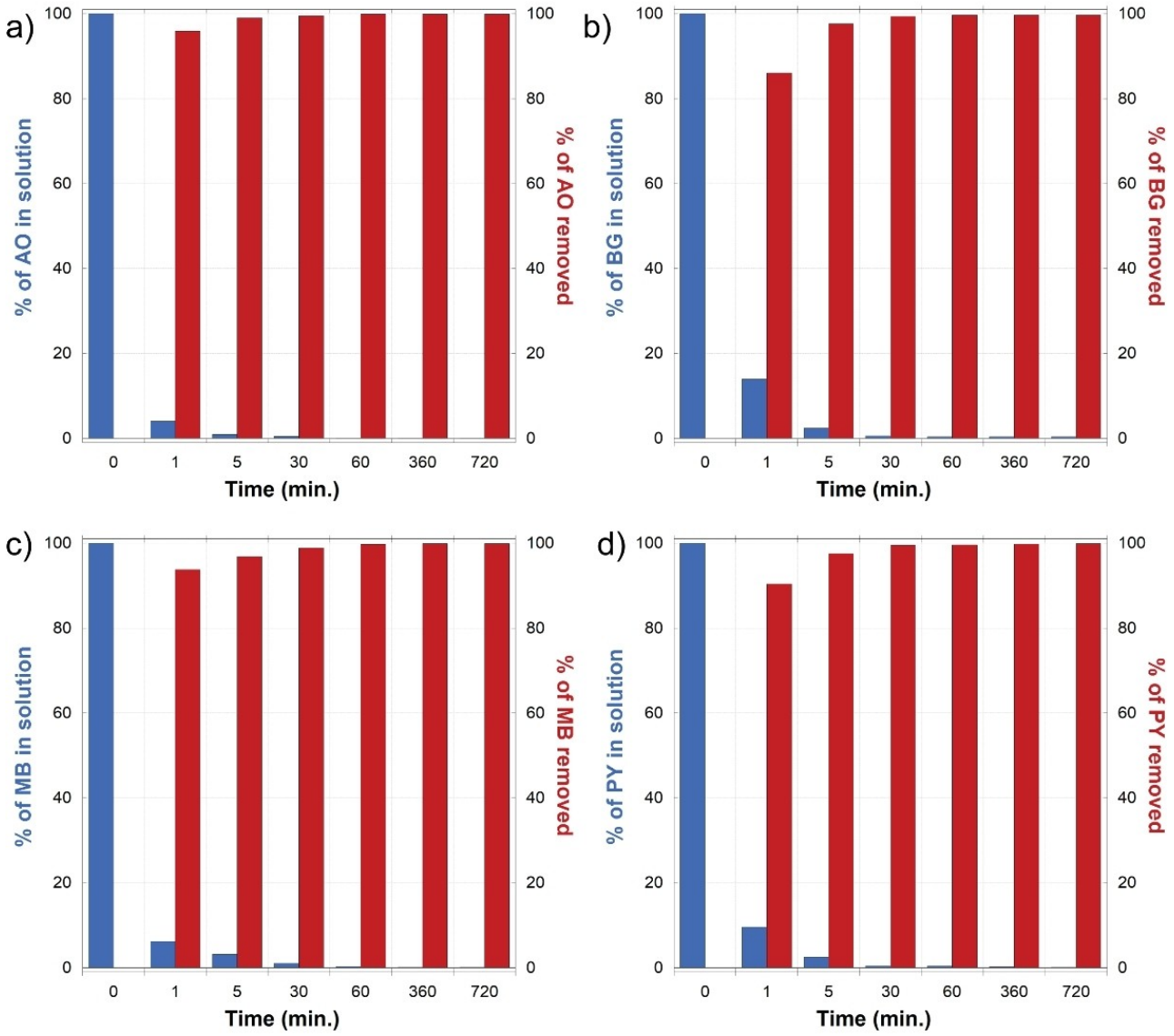

Figure 2. Evolution with time of the adsorption of AO (a), BG (b), MB (c) and PY (d) in 10 ppm solutions using real water samples from Turia river (50 mg of pellets of **1** as adsorbent). Blue bars represent the % of each dye within the solution and red bars represent the % of the dye removed from the solution.

crystals of **1** were soaked in saturated acetonitrile solutions of each organic dye for one week. After that period, we could obtain crystals of enough quality to solve the crystal structure of four host-guest systems by means of single-crystal X-ray diffraction (Table S1). Their formula, supported by CHSN elemental analysis, inductively coupled plasma mass spectrometry (ICP-MS) and thermogravimetric analysis (TGA) (see Experimental Section, Supporting Information), are: AO@{$Sr^{II}Cu_6^{II}$[(*S,S*)-methox]$_3(OH)_2(H_2O)$}$\cdot 6H_2O$ (**AO@1**), BG@{$Sr^{II}Cu_6^{II}$[(*S,S*)-methox]$_3(OH)_2(H_2O)$}$\cdot 5H_2O$ (**BG@1**), MB@{$Sr^{II}Cu_6^{II}$[(*S,S*)-methox]$_3(OH)_2(H_2O)$}$\cdot 6H_2O$ (**MB@1**) and PY@{$Sr^{II}Cu_6^{II}$[(*S,S*)-methox]$_3(OH)_2(H_2O)$}$\cdot 6H_2O$ (**PY@1**). Resolution of the crystal structure of adsorbates allowed the atomically-precise visualization of the main host-guest interactions, likely at the origin of the efficient captures of pollutant dyes by thio-alkyl residues decorating the framework (Figures 4, 5 and S8-S14).

The four compounds **AO@1**, **BG@1**, **MB@1** and **PY@1** are isomorphous to **1**, crystallizing in the $P6_3$ chiral space group of the hexagonal system. This behavior confirms the robustness of **1** as hosting matrix. They are built by uni-nodal **acs** six-connected three-dimensional (3D) strontium(II)-copper(II) porous networks, decorated by highly flexible $CH_2CH_2SCH_3$ thio-alkyl chains, which are capable to act as receptors towards guest dyes (Figures 3–5, S9, S11 and S13). The four crystal structures undoubtedly evidence that AO, BG, MB and PY guest molecules are encapsulated in the nanopores of **1**, where they are recognized by the thioether arms of the methionine residues. As expected for loaded-porous structures, dye molecules displayed a severe disorder in pores, both dynamical and statistic (see Experimental Section, Supporting Information). All the crystal structures exhibit different allocations of guests, with a 1:3 statistical distribution (Figures S8, S10, S12 and S14),

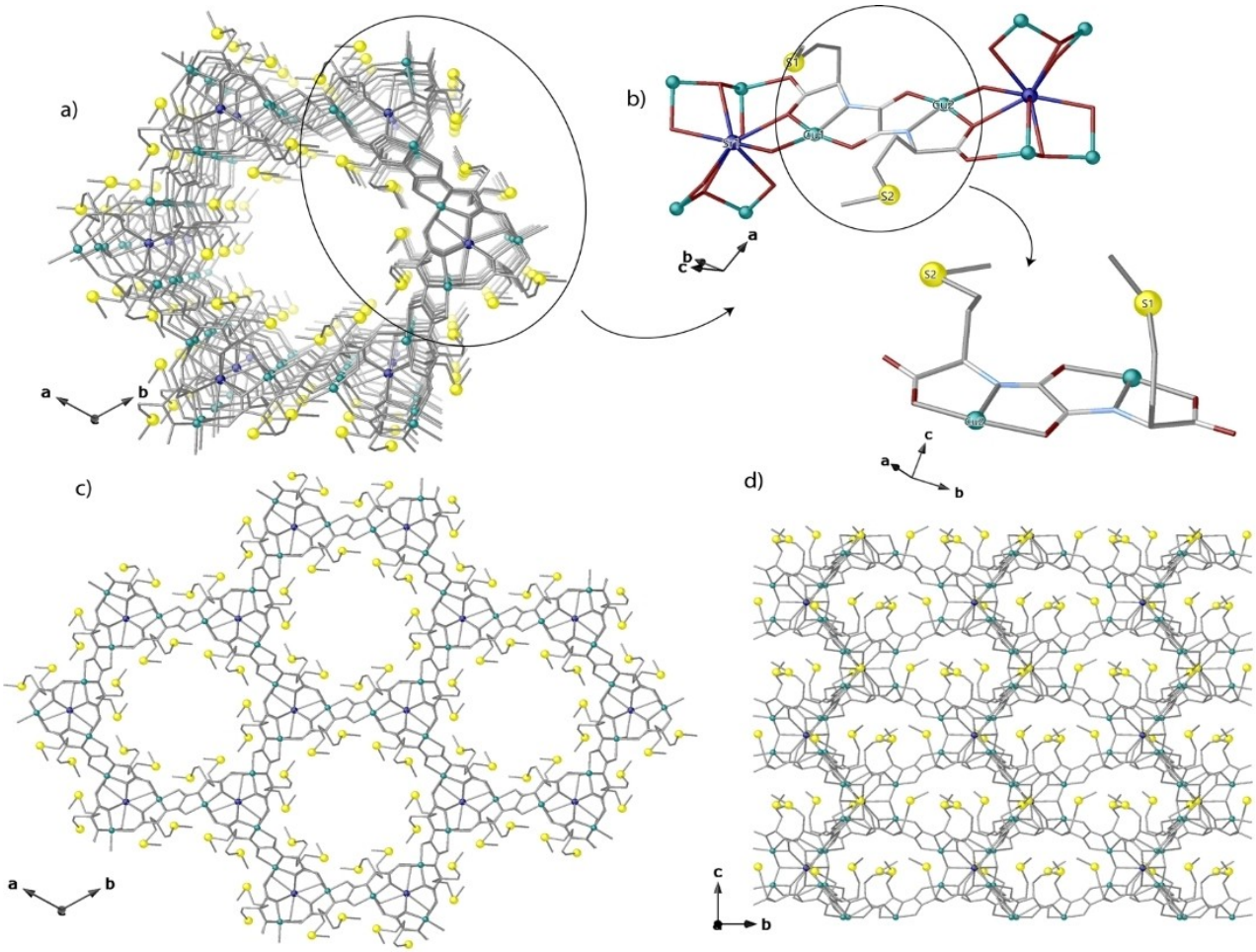

Figure 3. Crystal structure of **1**: (a) Perspective view along *c* crystallographic axis of a single channel in crystal structure of **1**. b) Fragments of **1** showing the dianionic bis(hydroxo) dicopper(II) building blocks. Views of a fragment of **1** in the *ab* (c) and *bc* (d) planes, respectively. Copper, strontium and sulfur atoms are represented by cyan, blue and yellow spheres, respectively, whereas the ligands (except sulfur) are depicted as sticks (carbon: gray, oxygen: red and nitrogen: blue).

strictly dependent on the size and chemical nature of the dye. The main host-guest interactions are assured by sulfur atoms directly interacting either with Cl^- anions in **AO@1**, **MB@1** and **PY@1** or with aromatic rings via the low-lying σ* orbitals of the C–S bond (σ-hole) -available for interaction with electron donors such as the four dyes π-systems.

As far as **AO@1**, **MB@1** and **PY@1** is concerned, the capture of Cl^- anions, nicely blocked in the most hindered voids of the MOF by direct S···Cl interactions [2.43(3), 2.20(2) and 2.87(2) Å, for **AO@1**, **MB@1** and **PY@1**, respectively], can be seen as a driving force for the further insertion of cationic dye molecules, which are captured thanks to S···π interactions, as well as also supported by those electrostatic interactions (Figures 5, S11 and S13).

In **AO@1** and **PY@1** the hosting network displayed a more open structure when compared with **MB@1** and especially with **BG@1**. The bigger size and/or less efficient packing of the latter dyes likely accounting for that. Indeed, in **PY@1** methionine arms are distended and interact through S···H–C weak interactions [shortest S···H–C distances of 2.88(3) and 3.16(3) Å], which anchor external aromatic rings to the walls of the MOF. The severe statistic and thermal disorder did not allow us to model terminal $-N(CH_3)_2$ (see Experimental Section for details). However, their defined orientations gave clues on potential C–H···N intermolecular interactions involving adjacent molecules. Indeed, supramolecular chains of Pyronin Y molecules evidence a propagation along the direction of channels, as imposed by the hosting matrix, which not only host but also align guests.

More evident σ-hole interactions are detected in **AO@1** crystal structure, where $-CH_2CH_2SCH_3$ methionine arms point toward the $-NH_2^+$ group of the Auramine O organic dye [S···N distance of 4.44(3) Å] (Figure 5). Further stabilizing host-guest interactions occur between $-CH_2CH_2SCH_3$ ethylthiomethyl chains and aromatic rings of AO dye molecule [centroid···C distances of 3.40(2), 3.56(2) and 3.72(2) Å] (Figure 5). Despite the unresolved disorder -that does not allow to spot any further detail and neither defining the messy $-N(CH_3)_2$ terminal group of the organic dye and a lattice water molecule-, it can be inferred implications of the free rotation of the two phenyl rings

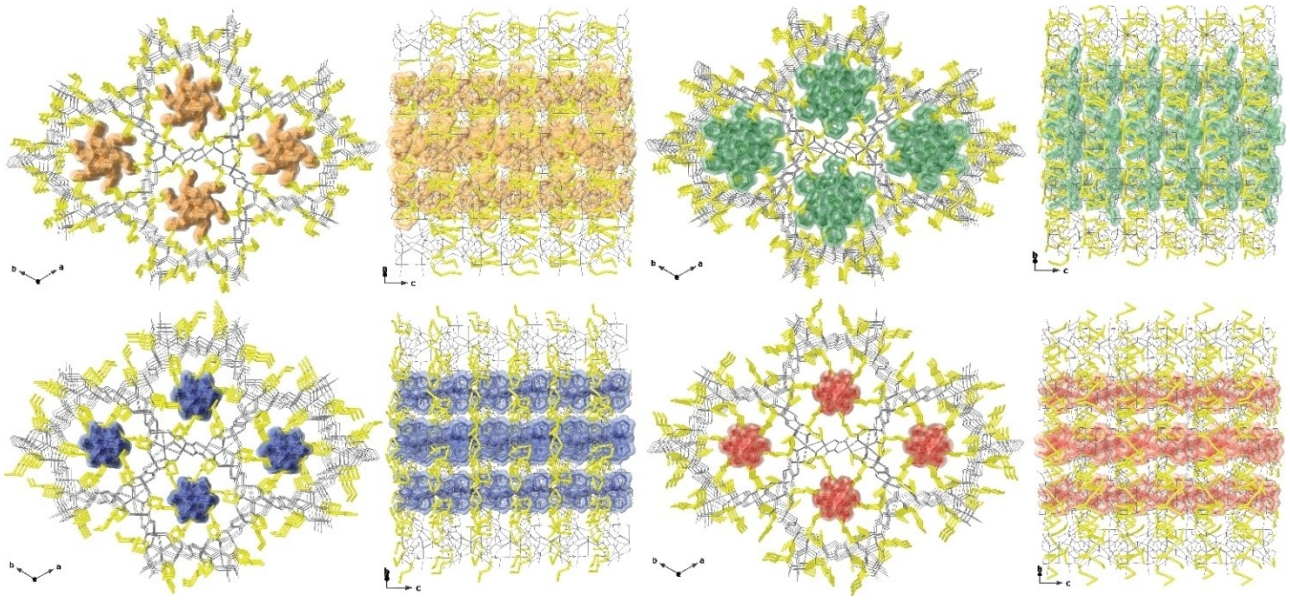

Figure 4. Perspective views in the *ab* (left) and *bc* (right) planes of the host-guest assemblies of **AO@1** (a), **BG@1** (b), **MB@1** (c) and **PY@1** (d). The networks are represented as light gray sticks with $-CH_2CH_2SCH_3$ ethylthiomethyl residues as yellow sticks and guest organic dyes as orange (AO), green (BG), blue (MB) and red (PY) solid surfaces. Free water molecules have been omitted for clarity.

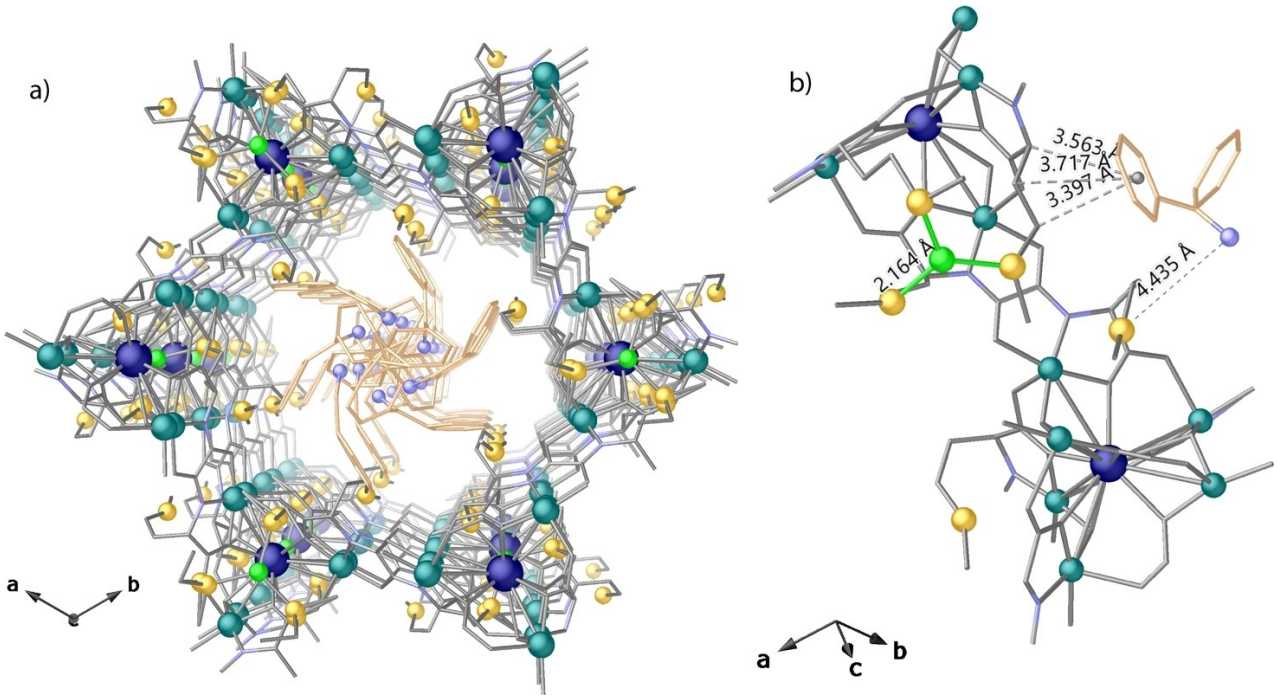

Figure 5. Details of host-guest interactions in **AO@1**: (a) Perspective view of a single channel of X-ray crystal structure of **AO@1** along *c* crystallographic axis emphasizing pores filled by Auramine O and (b) details of host-guest interactions (S···Cl and AO···S represented as green and grey dashed lines, respectively). Copper and calcium are represented by cyan and blue spheres respectively, whereas the ligands and guest molecules are depicted as grey and gold sticks except for sulfur atoms of methox moieties and nitrogen atoms of guest' molecule, which are represented by yellow and blue-sky spheres, respectively. Free water molecules are omitted for clarity.

in reducing the strength of the interactions, which, even if detected, it appears weak when looking at distances -although they must be imagined as averaged in the crystal.

In **BG@1** and **MB@1** crystal structures, the size of BG and MB and/or their worst self-packing impose a more contracted conformation of the methionine derivatives arms. BG crystal structure, exhibits a very nice interlock between BG molecules

and hosting matrix, based on S···π interactions [centroid···C distance of 3.14(3) Å] (Figure S9). As far as for **MB@1** is concerned, we have to underline a direct bond involving methionine-sulfur and nitrogen atoms belonging to the MB molecule at a distance of 1.79(2) Å, in agreement with similar bonds reported in literature,[15] which also confines sulfur atoms of the dye molecule at the center of the pores (Figure S11). Also, in both cases, due to dynamic disorder, terminal –N-$(CH_2CH_3)_2$ groups present in **BG@1** and –$N(CH_3)_2$ in **MB@1** have not been modelled (see Experimental Section for details). However, the core of the dye molecules -although with disorder- has been defined, suggesting the main interactions with terminal –$N(CH_2CH_3)_2$ and –$N(CH_3)_2$ groups likely involve dye intermolecular ones. Surprisingly, for all dyes, the high degree of loading in the confined space is the same. Each dye molecule does displace almost all water molecules from pores in order to reach the observed close-packing. The fact that channels are completely filled by organic dyes, makes the adsorbates very stable at air and room temperature for months.

The good capture performance of **1** for chosen dyes could be understood analyzing non-covalent interactions within the final aggregates with the help of X-ray crystallography. As stated above, it is known that σ-hole bonds play a pivotal role in the 3D organization of crystalline structures and in various molecular scaffolds. Indeed, these interactions, frequently unnoticed or identified as secondary contacts, can be highly predictable and are generally present. In this work, we considered and used them as a novel and efficient tool to reach high performance in capture of pollutant dyes. Studies on this subject have worked dramatically to interpret and rationalize properties of **1**. In fact, the importance of such interactions is clearly manifested in a multitude of biological phenomena.[82] In all the four adsorbates **AO@1**, **BG@1**, **MB@1** and **PY@1** a kind of S···π interactions, together with S···Cl interactions in **AO@1**, **MB@1** and **PY@1**, have been detected. Certainly, although an aromatic π-system can be electron-rich or electron-deficient, it can be non-covalently bonded to a σ-hole-containing molecule -as in the cases reported here containing molecule···π-system interactions. The σ-hole term is assigned to the area of positive, or less negative, electrostatic potential emerging on the outer surface of the covalently bonded sulfur atom. In this scenario, σ-hole interactions found in **AO@1**, **BG@1**, **MB@1** and **PY@1**, even if different in nature and discussed in the context of other electrostatic interactions, are the main forces at the origin of the efficient capture of dyes in **1**. Their density of propagation, through the confined space ensured by **1**, represent the power of encapsulation of the system, being reminiscent of peptide-based methionine. In such supramolecular aggregates, these bonds rely, to a large extent, also on polarization and charge transfer effects, accompanied by dispersive forces -even if the precise mix of these different components varies from one bond to another. Thus, it is clear that a particular sort of hole does not have to be present in the isolated monomer, but it will be active when cooperative and polarizing forces can occur.

Thermogravimetric Analysis, N_2 Isotherm Adsorption and X-Ray Powder Diffraction

The water content of **1**, **AO@1**, **BG@1**, **MB@1** and **PY@1** was determined by thermogravimetric analysis (TGA) under a dry N_2 atmosphere. All of them show a small loss of solvent from room temperature, in comparison with **1**, which agrees with the fact that the channels are filled with organic dyes. In particular, they showed a weight loss of 15.86 (**1**), 5.30 (**AO@1**), 4.35 (**BG@1**), 5.25 (**MB@1**) and 5.22% (**PY@1**), that correspond with 16, 6, 5, 6 and 6 water molecules, respectively, which is in line with CHSN analyses (Figure S15). The N_2 adsorption at 77 K of **AO@1**, **BG@1**, **MB@1** and **PY@1** showed a considerable reduction with respect to **1**, which further support that the channels are occupied by organic dyes molecules (Figure S16). The experimental powder X-ray diffraction (PXRD) patterns of polycrystalline samples of **1**, **AO@1**, **BG@1**, **MB@1** and **PY@1** confirm the purity and homogeneity of the bulk samples (Figure S17). As it was previously observed, the slight increase in relative intensity at the higher-angle peaks of dyes@**1**, with respect to **1**, are most likely consequence of the increase of the electronic density in the channels filled with organic dyes.

Conclusions

Herein, we have presented our recent advances on the relevance of σ-hole interactions toward applications. In particular, we have gained insight by means of single-crystal X-ray crystallography of the importance of such poorly investigated interactions for the removal of four organic dyes from real river waters. In doing so, we have precisely characterized four host-guest adsorbates, where the main interactions between the organic dyes and the framework allowed us to rationalize the appealing removal properties of **1**. Indeed, **1** has revealed as one of the best performing MOFs - in terms of both speed and removal efficiency - for the capture of organic dyes.[71] In an indirect manner, we have taken this MOF one step closer to real world applications by both its structuration as extruded pellets and the scale-up synthesis. This work represents an interesting beginning of a research line, which currently we are developing to integrate **1** in a decontamination pilot plant.

Data AvailabilityStatement

The data that support the findings of this study are available in the supplementary material of this article.

Deposition Numbers CCDC-2132442 (for **1**), CCDC-2132443 (for **AO@1**), CCDC-2132444 (for **BG@1**), CCDC-2132445 (for **MB@1**) and CCDC-2132446 (for **PY@1**) contain the supplementary crystallographic data for this paper. These data are provided free of charge by the joint Cambridge Crystallographic Data Centre and Fachinformationszentrum Karlsruhe Access Structures service.

Acknowledgements

This work was supported by the Ministerio de Ciencia e Innovación (Spain) (Projects PID2019-104778GB-I00 and Excellence Unit "Maria de Maeztu" CEX2019-000919-M), the Generalitat Valenciana (Project PROMETEO/2021/054) and the Ministero dell'Istruzione, dell'Università e della Ricerca (Italy). R. B. thank Fondazione CARIPLO (Project code: 2019-2090, "Economia Circolare: ricerca per un futuro sostenibile" 2019, MOCA) for postoctoral grant. Thanks are also extended to the "2019 Postdoctoral Junior Leader-Retaining Fellowship, la Caixa Foundation (ID100010434 and fellowship code LCF/BQ/PR19/11700011", "Subvenciones concedidas a la excelencia científica de juniors investigadores, SEJI/2020/034" and "Ramon y Cajal Programme (RYC2019-027940-I)" (J. F.-S.). E.P. acknowledges the financial support of the European Research Council under the European Union's Horizon2020 research and innovation programme/ERC Grant Agreement No 814804, MOF-reactors.

Conflict of Interest

The authors declare no conflict of interest.

Data Availability Statement

The data that support the findings of this study are available from the corresponding author upon reasonable request.

Keywords: host-guest chemistry · metal-organic frameworks · organic dyes · σ-Hole Interaction · water remediation

[1] J.-M. Lehn, *Supramol. Chem.*, Wiley, **1995**.
[2] G. Vantomme, E. W. Meijer, *Science* **2019**, *363*, 1396–1397.
[3] D. B. Amabilino, P. A. Gale, *Chem. Soc. Rev.* **2017**, *46*, 2376–2377.
[4] W. Liu, J. F. Stoddart, *Chem* **2021**, *7*, 919–947.
[5] J. S. Murray, P. Lane, P. Politzer, *Int. J. Quantum Chem.* **2008**, *108*, 2770–2781.
[6] S. Scheiner, U. Adhikari, *J. Phys. Chem. A* **2011**, *115*, 11101–11110.
[7] P. Politzer, J. S. Murray, T. Clark, *Phys. Chem. Chem. Phys.* **2013**, *15*, 11178.
[8] A. Obata, H. Kawazura, H. Miyamae, *Acta Crystallogr. Sect. C Cryst. Struct. Commun.* **1984**, *40*, 45–48.
[9] Y. Nagao, T. Hirata, S. Goto, S. Sano, A. Kakehi, K. Iizuka, M. Shiro, *J. Am. Chem. Soc.* **1998**, *120*, 3104–3110.
[10] M. Iwaoka, S. Takemoto, S. Tomoda, *J. Am. Chem. Soc.* **2002**, *124*, 10613–10620.
[11] B. M. Hudson, E. Nguyen, D. J. Tantillo, *Org. Biomol. Chem.* **2016**, *14*, 3975–3980.
[12] S. P. Thomas, D. Jayatilaka, T. N. Guru Row, *Phys. Chem. Chem. Phys.* **2015**, *17*, 25411–25420.
[13] M. Mon, J. Ferrando-Soria, T. Grancha, F. R. Fortea-Pérez, J. Gascon, A. Leyva-Pérez, D. Armentano, E. Pardo, *J. Am. Chem. Soc.* **2016**, *138*, 7864–7867.
[14] M. Mon, F. Lloret, J. Ferrando-Soria, C. Martí-Gastaldo, D. Armentano, E. Pardo, *Angew. Chem. Int. Ed.* **2016**, *55*, 11167–11172; *Angew. Chem.* **2016**, *128*, 11333–11338.
[15] M. Mon, R. Bruno, E. Tiburcio, M. Viciano-Chumillas, L. H. G. Kalinke, J. Ferrando-Soria, D. Armentano, E. Pardo, *J. Am. Chem. Soc.* **2019**, *141*, 13601–13609.
[16] M. Mon, X. Qu, J. Ferrando-Soria, I. Pellicer-Carreño, A. Sepúlveda-Escribano, E. V. Ramos-Fernandez, J. C. Jansen, D. Armentano, E. Pardo, *J. Mater. Chem. A* **2017**, *5*, 20120–20125.
[17] M. Mon, M. A. Rivero-Crespo, J. Ferrando-Soria, A. Vidal-Moya, M. Boronat, A. Leyva-Pérez, A. Corma, J. C. Hernández-Garrido, M. López-Haro, J. J. Calvino, G. Ragazzon, A. Credi, D. Armentano, E. Pardo, *Angew. Chem. Int. Ed.* **2018**, *57*, 6186–6191; *Angew. Chem.* **2018**, *130*, 6294–6299.
[18] C. Negro, H. Martínez Pérez-Cejuela, E. F. Simó-Alfonso, J. M. Herrero-Martínez, R. Bruno, D. Armentano, J. Ferrando-Soria, E. Pardo, *ACS Appl. Mater. Interfaces* **2021**, *13*, 28424–28432.
[19] R. Bruno, M. Mon, P. Escamilla, J. Ferrando-Soria, E. Esposito, A. Fuoco, M. Monteleone, J. C. Jansen, R. Elliani, A. Tagarelli, D. Armentano, E. Pardo, *Adv. Funct. Mater.* **2021**, *31*, 2008499.
[20] E. Tiburcio, R. Greco, M. Mon, J. Ballesteros-Soberanas, J. Ferrando-Soria, M. López-Haro, J. C. Hernández-Garrido, J. Oliver-Meseguer, C. Marini, M. Boronat, D. Armentano, A. Leyva-Pérez, E. Pardo, *J. Am. Chem. Soc.* **2021**, *143*, 2581–2592.
[21] H. Furukawa, K. E. Cordova, M. O'Keeffe, O. M. Yaghi, *Science* **2013**, *341*, 974.
[22] H.-C. Zhou, S. Kitagawa, *Chem. Soc. Rev.* **2014**, *43*, 5415–5418.
[23] B. Seoane, S. Castellanos, A. Dikhtiarenko, F. Kapteijn, J. Gascon, *Coord. Chem. Rev.* **2016**, *307*, 147–187.
[24] G. Maurin, C. Serre, A. Cooper, G. Férey, *Chem. Soc. Rev.* **2017**, *46*, 3104–3107.
[25] O. M. Yaghi, M. J. Kalmutzki, C. S. Diercks, *Introduction to Reticular Chemistry*, Wiley, **2019**.
[26] X. Zhang, B. Wang, A. Alsalme, S. Xiang, Z. Zhang, B. Chen, *Coord. Chem. Rev.* **2020**, *423*, 213507.
[27] W. Xu, B. Tu, Q. Liu, Y. Shu, C.-C. Liang, C. S. Diercks, O. M. Yaghi, Y.-B. Zhang, H. Deng, Q. Li, *Nat. Rev. Mater.* **2020**, *5*, 764–779.
[28] R. Freund, O. Zaremba, G. Arnauts, R. Ameloot, G. Skorupskii, M. Dincă, A. Bavykina, J. Gascon, A. Ejsmont, J. Goscianska, M. Kalmutzki, U. Lächelt, E. Ploetz, C. S. Diercks, S. Wuttke, *Angew. Chem. Int. Ed.* **2021**, *60*, 23975–24001.
[29] H. Deng, S. Grunder, K. E. Cordova, C. Valente, H. Furukawa, M. Hmadeh, F. Gandara, A. C. Whalley, Z. Liu, S. Asahina, H. Kazumori, M. O'Keeffe, O. Terasakij, F. Stoddart, O. M. Yaghi, *Science* **2012**, *336*, 1018–1023.
[30] D. Antypov, A. Shkurenko, P. M. Bhatt, Y. Belmabkhout, K. Adil, A. Cadiau, M. Suyetin, M. Eddaoudi, M. J. Rosseinsky, M. S. Dyer, *Nat. Commun.* **2020**, *11*, 6099.
[31] Z. Ji, H. Wang, S. Canossa, S. Wuttke, O. M. Yaghi, *Adv. Funct. Mater.* **2020**, *30*, 2000238.
[32] H. Wang, Z. Shi, J. Yang, T. Sun, B. Rungtaweevoranit, H. Lyu, Y. Zhang, O. M. Yaghi, *Angew. Chem. Int. Ed.* **2021**, *60*, 3417–3421; *Angew. Chem.* **2021**, *133*, 3459–3463.
[33] M. Mon, R. Bruno, S. Sanz-Navarro, C. Negro, J. Ferrando-Soria, L. Bartella, L. Di Donna, M. Prejanò, T. Marino, A. Leyva-Pérez, D. Armentano, E. Pardo, *Nat. Commun.* **2020**, *11*, 3080.
[34] M. Mon, R. Bruno, E. Tiburcio, A. Grau-Atienza, A. Sepúlveda-Escribano, E. V. Ramos-Fernandez, A. Fuoco, E. Esposito, M. Monteleone, J. C. Jansen, J. Cano, J. Ferrando-Soria, D. Armentano, E. Pardo, *Chem. Mater.* **2019**, *31*, 5856–5866.
[35] M. Mon, R. Bruno, J. Ferrando-Soria, L. Bartella, L. Di Donna, M. Talia, R. Lappano, M. Maggiolini, D. Armentano, E. Pardo, *Mater. Horiz.* **2018**, *5*, 683–690.
[36] Y. Inokuma, T. Arai, M. Fujita, *Nat. Chem.* **2010**, *2*, 780–783.
[37] Y. Inokuma, S. Yoshioka, J. Ariyoshi, T. Arai, M. Fujita, *Nat. Protoc.* **2014**, *9*, 246–252.
[38] N. Zigon, M. Hoshino, S. Yoshioka, Y. Inokuma, M. Fujita, *Angew. Chem. Int. Ed.* **2015**, *54*, 9033–9037; *Angew. Chem.* **2015**, *127*, 9161–9165.
[39] V. Guillerm, M. Eddaoudi, *Acc. Chem. Res.* **2021**, *54*, 3298–3312.
[40] H. Jiang, D. Alezi, M. Eddaoudi, *Nat. Rev. Mater.* **2021**, *6*, 466–487.
[41] R. Freund, S. Canossa, S. M. Cohen, W. Yan, H. Deng, V. Guillerm, M. Eddaoudi, D. G. Madden, D. Fairen-Jimenez, H. Lyu, L. K. Macreadie, Z Ji, Y. Zhang, B. Wang, F. Haase, C. Wöll, O. Zaremba, J. Andreo, S. Wuttke, C. S. Diercks, *Angew. Chem. Int. Ed.* **2021**, *60*, 23946–23974.
[42] L. Feng, G. S. Day, K.-Y. Wang, S. Yuan, H.-C. Zhou, *Chem* **2020**, *6*, 2902–2923.
[43] Z. Chen, H. Jiang, M. Li, M. O'Keeffe, M. Eddaoudi, *Chem. Rev.* **2020**, *120*, 8039–8065.
[44] M. Li, D. Li, M. O'Keeffe, O. M. Yaghi, *Chem. Rev.* **2014**, *114*, 1343–1370.
[45] M. O'Keeffe, O. M. Yaghi, *Chem. Rev.* **2012**, *112*, 675–702.
[46] Y. Isaka, Y. Kawase, Y. Kuwahara, K. Mori, H. Yamashita, *Angew. Chem. Int. Ed.* **2019**, *58*, 5402–5406; *Angew. Chem.* **2019**, *131*, 5456–5460.

[47] H. Jiang, J. Jia, A. Shkurenko, Z. Chen, K. Adil, Y. Belmabkhout, L. J. Weselinski, A. H. Assen, D.-X. Xue, M. O'Keeffe, M. Eddaoudi, *J. Am. Chem. Soc.* **2018**, *140*, 8858–8867.
[48] P. Li, N. A. Vermeulen, C. D. Malliakas, D. A. Gómez-Gualdrón, A. J. Howarth, B. L. Mehdi, A. Dohnalkova, N. D. Browning, M. O'Keeffe, O. K. Farha, *Science* **2017**, *356*, 624–627.
[49] F. R. Fortea-Pérez, M. Mon, J. Ferrando-Soria, M. Boronat, A. Leyva-Pérez, A. Corma, J. M. Herrera, D. Osadchii, J. Gascon, D. Armentano, E. Pardo, *Nat. Mater.* **2017**, *16*, 760–766.
[50] R. Li, S. Alomari, T. Islamoglu, O. K. Farha, S. Fernando, S. M. Thagard, T. M. Holsen, M. Wriedt, *Environ. Sci. Technol.* **2021**, *55*, 15162–15171.
[51] Z. Jiang, X. Xu, Y. Ma, H. S. Cho, D. Ding, C. Wang, J. Wu, P. Oleynikov, M. Jia, J. Cheng, Y. Zhou, O. Terasaki, T. Peng, L. Zan, H. Deng, *Nature* **2020**, *586*, 549–554.
[52] M. Viciano-Chumillas, M. Mon, J. Ferrando-Soria, A. Corma, A. Leyva-Pérez, D. Armentano, E. Pardo, *Acc. Chem. Res.* **2020**, *53*, 520–531.
[53] R. J. Young, M. T. Huxley, E. Pardo, N. R. Champness, C. J. Sumby, C. J. Doonan, *Chem. Sci.* **2020**, *11*, 4031–4050.
[54] B. Wang, X.-L. Lv, D. Feng, L.-H. Xie, J. Zhang, M. Li, Y. Xie, J.-R. Li, H.-C. Zhou, *J. Am. Chem. Soc.* **2016**, *138*, 6204–6216.
[55] M. I. Gonzalez, A. B. Turkiewicz, L. E. Darago, J. Oktawiec, K. Bustillo, F. Grandjean, G. J. Long, J. R. Long, *Nature* **2020**, *577*, 64–68.
[56] N. Hanikel, M. S. Prévot, O. M. Yaghi, *Nat. Nanotechnol.* **2020**, *15*, 348–355.
[57] A. Bavykina, N. Kolobov, I. S. Khan, J. A. Bau, A. Ramirez, J. Gascon, *Chem. Rev.* **2020**, *120*, 8468–8535.
[58] Z. Chen, P. Li, R. Anderson, X. Wang, X. Zhang, L. Robison, L. R. Redfern, S. Moribe, T. Islamoglu, D. A. Gómez-Gualdrón, T. Yildirimj, F. Stoddart, O. K. Farha, *Science* **2020**, *368*, 297–303.
[59] R.-B. Lin, S. Xiang, W. Zhou, B. Chen, *Chem* **2020**, *6*, 337–363.
[60] L. S. Xie, G. Skorupskii, M. Dincă, *Chem. Rev.* **2020**, *120*, 8536–8580.
[61] Q. Hu, J. Yu, M. Liu, A. Liu, Z. Dou, Y. Yang, *J. Med. Chem.* **2014**, *57*, 5679–5685.
[62] M. Viciano-Chumillas, X. Liu, A. Leyva-Pérez, D. Armentano, J. Ferrando-Soria, E. Pardo, *Coord. Chem. Rev.* **2022**, *451*, 214273.
[63] W. M. Bloch, A. Burgun, C. J. Coghlan, R. Lee, M. L. Coote, C. J. Doonan, C. J. Sumby, *Nat. Chem.* **2014**, *6*, 906–912.
[64] W. M. Bloch, N. R. Champness, C. J. Doonan, *Angew. Chem. Int. Ed.* **2015**, *54*, 12860–12867; *Angew. Chem.* **2015**, *127*, 13052–13059.
[65] A. Burgun, C. J. Coghlan, D. M. Huang, W. Chen, S. Horike, S. Kitagawa, J. F. Alvino, G. F. Metha, C. J. Sumby, C. J. Doonan, *Angew. Chem. Int. Ed.* **2017**, *56*, 8412–8416; *Angew. Chem.* **2017**, *129*, 8532–8536.
[66] R.-W. Huang, Y.-S. Wei, X.-Y. Dong, X.-H. Wu, C.-X. Du, S.-Q. Zang, T. C. W. Mak, *Nat. Chem.* **2017**, *9*, 689–697.
[67] K. Rissanen, *Chem. Soc. Rev.* **2017**, *46*, 2638–2648.
[68] R. Adam, M. Mon, R. Greco, L. H. G. Kalinke, A. Vidal-Moya, A. Fernandez, R. E. P. Winpenny, A. Doménech-Carbó, A. Leyva-Pérez, D. Armentano, E. Pardo, J. Ferrando-Soria, *J. Am. Chem. Soc.* **2019**, *141*, 10350–10360.
[69] N. Hanikel, X. Pei, S. Chheda, H. Lyu, W. Jeong, J. Sauer, L. Gagliardi, O. M. Yaghi, *Science* **2021**, *374*, 454–459.
[70] A. Tkaczyk, K. Mitrowska, A. Posyniak, *Sci. Total Environ.* **2020**, *717*, 137222.
[71] M. Mon, R. Bruno, J. Ferrando-Soria, D. Armentano, E. Pardo, *J. Mater. Chem. A* **2018**, *6*, 4912–4947.
[72] A. Ahmad, S. H. Mohd-Setapar, C. S. Chuong, A. Khatoon, W. A. Wani, R. Kumar, M. Rafatullah, *RSC Adv.* **2015**, *5*, 30801–30818.
[73] E. Brillas, C. A. Martínez-Huitle, *Appl. Catal. B* **2015**, *166–167*, 603–643.
[74] T. He, X.-J. Kong, J.-R. Li, *Acc. Chem. Res.* **2021**, *54*, 3083–3094.
[75] X.-J. Kong, J.-R. Li, *Engineering* **2021**, *7*, 1115–1139.
[76] C.-C. Wang, J.-R. Li, X.-L. Lv, Y.-Q. Zhang, G. Guo, *Energy Environ. Sci.* **2014**, *7*, 2831–2867.
[77] D. Jiang, M. Chen, H. Wang, G. Zeng, D. Huang, M. Cheng, Y. Liu, W. Xue, Z. Wang, *Coord. Chem. Rev.* **2019**, *380*, 471–483.
[78] E. M. Dias, C. Petit, *J. Mater. Chem. A* **2015**, *3*, 22484–22506.
[79] Y. Wen, P. Zhang, V. K. Sharma, X. Ma, H.-C. Zhou, *Cell Reports Phys. Sci.* **2021**, *2*, 100348.
[80] M. Mon, R. Bruno, E. Tiburcio, P.-E. Casteran, J. Ferrando-Soria, D. Armentano, E. Pardo, *Chem. Eur. J.* **2018**, *24*, 17712–17718.
[81] A. Knebel, A. Bavykina, S. J. Datta, L. Sundermann, L. Garzon-Tovar, Y. Lebedev, S. Durini, R. Ahmad, S. M. Kozlov, G. Shterk, M. Karunakaran, I. D. Carja, D. Simic, I. Weilert, M. Klüppel, U. Giese, L. Cavallo, M. Rueping, M. Eddaoudi, J. Caro, Jorge Gascon, *Nat. Mater.* **2020**, *19*, 1346–1353.
[82] M. S. Smith, E. E. K. Lawrence, W. M. Billings, K. S. Larsen, N. A. Bécar, J. L. Price, *ACS Chem. Biol.* **2017**, *12*, 2535–2537.

Manuscript received: January 10, 2022
Accepted manuscript online: February 21, 2022
Version of record online: March 24, 2022